



ISSN 0975-413X
CODEN (USA): PCHHAX

Der Pharma Chemica, 2016, 8(2):476-487
(<http://derpharmachemica.com/archive.html>)

A theoretical analysis of the inhibition of the VEGFR-2 vascular endothelial growth factor and the anti-proliferative activity against the HepG2 hepatocellular carcinoma cell line by a series of 1-(4-((2-oxoindolin-3-ylidene)amino)phenyl)-3-arylureas

Juan S. Gómez-Jeria* and Ítalo Orellana

Quantum Pharmacology Unit, Department of Chemistry, Faculty of Sciences, University of Chile. Las Palmeras 3425, Santiago, Chile

ABSTRACT

An analysis of the relationships between electronic structure and the inhibition of the kinase activity of VEGFR-2 was carried out for a series of 1-(4-((2-oxoindolin-3-ylidene)amino)phenyl)-3-arylureas. A similar study was done for the case of cytotoxicity against the HepG2 liver cancer cell line. The Klopman-Peradejordi-Gómez formal method was used. The local atomic reactivity indices were obtained at the B3LYP/6-31G(d,p) level after full geometry optimization. Statistically significant equations relating several local atomic reactivity indices with both activities were obtained. From the results, the corresponding partial 2D pharmacophores were built, containing several sites that can be used for substitution for enhancing affinity.

Keywords: KPG method, QSAR, HepG2 cells, DFT, VEGFR-2 receptor.

INTRODUCTION

During the search of molecular systems endowed with biological activities to be studied with the Klopman-Peradejordi-Gómez (KPG) method, we found a series of 1-(4-((2-oxoindolin-3-ylidene)amino)phenyl)-3-arylureas possessing the ability to inhibit the kinase activity of the vascular endothelial growth factor receptor-2 (VEGFR-2), and also a cytotoxic activity against the HepG2 hepatocellular carcinoma cell line [1]. VEGFR2 is vital for the functions of vascular endothelial cells (vascular development and regulation of vascular permeability). The discovery of inhibitors blocking the autophosphorylation of VEGFR-2 created new tools for the possible treatment of diverse cancers [1-22]. On the other hand, the development of new molecules with cytotoxicity against particular kinds of cells is also a tool to fight cancer [23-28]. Here we present the results of a search for relationships between the electronic structure of this series of 1-(4-((2-oxoindolin-3-ylidene)amino)phenyl)-3-arylureas and the abovementioned biological activities. The local atomic reactivity indices (LARIs) obtained in this study and others are been used to create a large database to explore the possibility of assigning “standard” values for atoms usually found in QSAR studies.

MATERIALS AND METHODS

The method employed here to obtain relationships between the electronic structure and biological activity is the only member of the *formal* methods class [30]. It is essentially grounded on the statistical-mechanical definition of the equilibrium constant and Klopman's formula for the interaction energy between two molecular systems (ΔE) [31, 32]. The first version of this model was employed by Peradejordi et al., Tomás and Aulló and myself [33-41]. It gave very good results for several different kinds of molecules and receptors. During the 1980's the interaction energy expression was expanded to include by separate the contribution of the molecular orbitals [42]. During year 2002 the conceptual basis for obtaining the orientational parameter of the substituents was published [43]. These developments led to very good results. Also, the method was improved by suggesting a new way to build the data matrix. The last theoretical advance was completed during year 2012 when new local atomic reactivity indices were obtained from the ΔE expression [44]. Also, during year 2012 a breakthrough was achieved when it was demonstrated that the method can be applied successfully to any biological activity [45, 46]. From this moment the application of the Klopman-Peradejordi-Gómez method (KPG) to very different molecules and biological activities produced surprisingly good results ([47-64] and references therein). Considering that the formula has been presented and explained in detail in many publications, we shall discuss only the resulting equations.

Selection of molecules and biological activities.

The selected molecules are a group of series of 1-(4-((2-oxoindolin-3-ylidene)amino)phenyl)-3-arylureas that were selected from a recent study [1]. The biological activities analyzed here are the reported experimental results for the *in vitro* cytotoxic activity against HepG2 liver cancer cells and the inhibitory activity against VEGFR-2. The general formula and biological activity of the selected molecules are displayed, respectively, in Fig. 1 and Table 2.

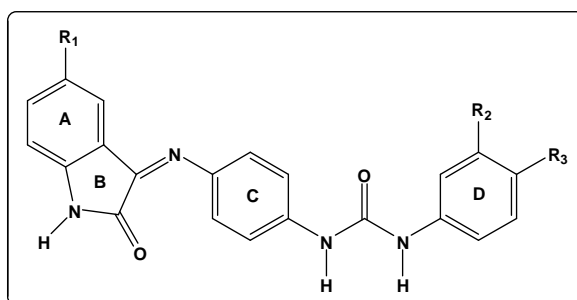


Figure 1. General formulas of the series of 1-(4-((2-oxoindolin-3-ylidene)amino)phenyl)-3-arylureas

Table 1. 1-(4-((2-oxoindolin-3-ylidene)amino)phenyl)-3-arylurea series and biological activities

Mol.	R ₁	R ₂	R ₃	log(IC ₅₀) HepG2	log(IC ₅₀) VEGFR2
1	H	H	H	0.54	0.75
2	H	CF ₃	H	0.48	0.63
3	H	H	CN	0.89	0.71
4	H	H	F	1.00	---
5	H	Cl	H	0.51	0.41
6	H	H	Cl	0.49	0.40
7	H	H	SO ₂ NH ₂	1.07	---
8	F	H	H	1.35	---
9	F	CF ₃	H	0.43	0.33
10	F	H	F	1.49	---
11	F	Cl	H	0.36	0.30
12	F	H	Cl	0.26	0.29
13	F	H	OMe	0.45	0.43
14	F	H	SO ₂ NH ₂	1.14	---
15	Cl	H	H	1.33	---
16	Cl	CF ₃	H	1.01	---
17	Cl	H	F	0.50	0.59
18	Cl	Cl	H	0.47	-0.12
19	Cl	H	Cl	0.92	-0.15
20	Cl	H	OMe	1.35	---
21	Cl	H	SO ₂ NH ₂	0.50	-0.51

Calculations.

The electronic structure of all molecules was calculated within the Density Functional Theory (DFT) at the B3LYP/6-31g(d,p) level with full geometry optimization. The Gaussian 03 suite of programs was used [65]. No attempt to verify if the conformation obtained corresponds to the absolute minimum. But, unless a molecular interaction occurs in the final structure, the value of the LARIs should not noticeably change. All the information needed to calculate numerical values for the local atomic reactivity indices was obtained from the Gaussian results with the D-Cent-QSAR software [66]. All the electron populations smaller than or equal to 0.01 e were considered as zero [44]. Negative electron populations coming from Mulliken Population Analysis were corrected as usual [67]. Since the resolution of the system of linear equations is not possible because we have not enough molecules, we employed Linear Multiple Regression Analysis (LMRA) techniques to find the best solution. For each case, a matrix containing the dependent variable (the biological activity) and the local atomic reactivity indices of all atoms of the common skeleton as independent variables was built (see [68] for details about the building of data matrix). The Statistica software was used for LMRA [69]. We worked with the *common skeleton hypothesis* stating that there is a definite collection of atoms, common to all molecules analyzed, that accounts for nearly all the biological activity. The action of the substituents consists in modifying the electronic structure of the common skeleton and influencing the right alignment of the drug throughout the orientational parameters. It is hypothesized that different parts or this common skeleton accounts for almost all the interactions leading to the expression of a given biological activity. The common skeleton for the series of 1-(4-((2-oxoindolin-3-ylidene)amino)phenyl)-3-arylureas is shown in Fig. 2.

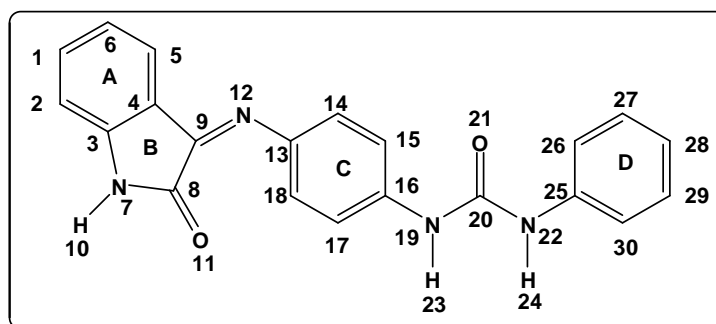


Figure 2. Common skeleton of the series of 1-(4-((2-oxoindolin-3-ylidene)amino)phenyl)-3-arylureas

RESULTS

In vitro cytotoxic activity against HepG2 liver cancer cells.

No statistically significant equation was found for $n=21$. Therefore, we removed the highest experimental values, one by one, until a satisfactory equation was obtained. The basis of this procedure is the hypothesis stating that, after a certain value, the mechanism of cytotoxicity changes. Finally, the best equation obtained was:

$$\log(IC_{50}) = 9.42 + 1.29F_{27}(HOMO)^* + 2.44F_{18}(HOMO - 1)^* - 0.004S_{18}^N(LUMO)^* + 0.59S_{11}^E - 0.002S_{17}^N(LUMO + 2)^* \quad (1)$$

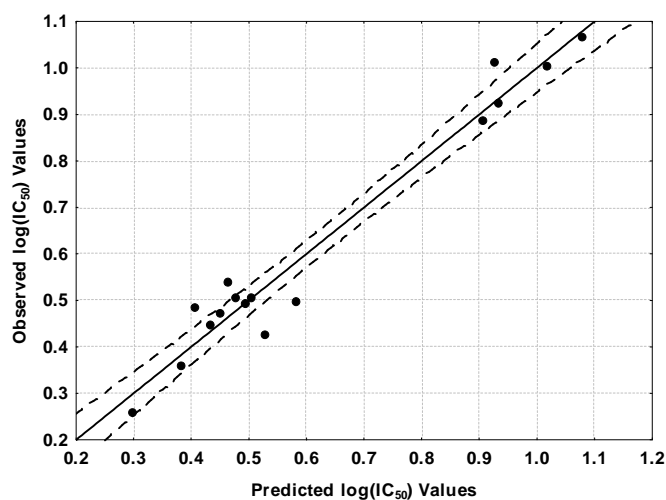
with $n=16$, $R=0.98$, $R^2=0.96$, $\text{adj-}R^2=0.94$, $F(5,10)=49.03$ ($p<0.000001$) and $SD=0.06$. No outliers were detected and no residuals fall outside the $\pm 2\sigma$ limits. Here, $F_{27}(HOMO)^*$ is the Fukui index of the highest occupied MO localized on atom 27, $F_{18}(HOMO - 1)^*$ is the Fukui index of the second highest occupied MO localized on atom 18, $S_{18}^N(LUMO)^*$ is the nucleophilic superdelocalizability of the lowest vacant MO localized on atom 18, S_{11}^E is the total atomic electrophilic superdelocalizability of atom 11 and $S_{17}^N(LUMO + 2)^*$ is the nucleophilic superdelocalizability of the third lowest vacant MO localized on atom 17. Tables 2 and 3 show the beta coefficients, the results of the t-test for significance of coefficients and the matrix of squared correlation coefficients for the variables of Eq. 1. There are no significant internal correlations between independent variables (Table 3). Figure 3 displays the plot of observed vs. calculated $\log(IC_{50})$ values.

Table 2. Beta coefficients and t-test for significance of coefficients in Eq. 1

Var.	Beta	t(10)	p-level
$F_{27}(HOMO)^*$	0.56	8.38	<0.000008
$F_{18}(HOMO-1)^*$	0.57	8.83	<0.000005
$S_{18}^N(LUMO)^*$	-0.65	-9.12	<0.000004
S_{11}^E	0.48	6.84	<0.00005
$S_{17}^N(LUMO+2)^*$	-0.32	-4.85	<0.0007

Table 3. Matrix of squared correlation coefficients for the variables in Eq. 1

	$F_{27}(HOMO)^*$	$F_{18}(HOMO-1)^*$	$S_{18}^N(LUMO)^*$	S_{11}^E
$F_{18}(HOMO-1)^*$	0.002	1		
$S_{18}^N(LUMO)^*$	0.04	0.03	1	
S_{11}^E	0.08	0.008	0.10	1
$S_{17}^N(LUMO+2)^*$	0.02	0.0009	0.05	0.02

Figure 3. Plot of predicted vs. observed $\log(IC_{50})$ values (Eq. 1). Dashed lines denote the 95% confidence interval

The associated statistical parameters of Eq. 1 indicate that this equation is statistically significant and that the variation of the numerical values of a group of five local atomic reactivity indices of atoms of the common skeleton explains about 94% of the variation of $\log(IC_{50})$ in this series of 1-(4-((2-oxoindolin-3-ylidene)amino)phenyl)-3-arylureas. Figure 3, spanning about 1.0 order of magnitude, shows that there is a good correlation of observed versus calculated values and that almost all points are inside the 95% confidence interval. This can be considered as an indirect evidence that the common skeleton hypothesis works relatively well for this set of molecules. A very important point to stress is the following. When a local atomic reactivity index of an inner occupied MO (i.e., HOMO-1 and/or HOMO-2) or of a higher vacant MO (LUMO+1 and/or LUMO+2) appears in any equation, this means that the remaining of the upper occupied MOs (for example, if HOMO-2 appears, upper means HOMO-1 and

HOMO) or the remaining of the empty MOs (for example, if LUMO+1 appears, lower means the LUMO) contribute to the interaction. Their absence in the equation only means that the variation of their numerical values does not account for the variation of the numerical value of the biological property.

Inhibitory activity against VEGFR-2.

The best equation obtained was:

$$\log(IC_{50}) = 1.79 + 0.004S_6^N(LUMO + 2)^* - 0.16S_{26}^E(HOMO - 2)^* + 0.58F_{21}(HOMO - 2)^* - 0.28\eta_{30} \quad (2)$$

with $n=13$, $R=0.99$, $R^2=0.99$, $\text{adj-}R^2=0.98$, $F(4,8)=171.26$ ($p<0.000001$) and $SD=0.05$. No outliers were detected and no residuals fall outside the $\pm 2\sigma$ limits. Here, $S_6^N(LUMO + 2)^*$ is the nucleophilic superdelocalizability of the third lowest vacant MO localized on atom 6, $S_{26}^E(HOMO - 2)^*$ is the electrophilic superdelocalizability of the third highest occupied MO localized on atom 26, $F_{21}(HOMO - 2)^*$ is the Fukui index of the third highest occupied MO localized on atom 21 and η_{30} is the local atomic hardness of atom 30. Tables 4 and 5 show the beta coefficients, the results of the t-test for significance of coefficients and the matrix of squared correlation coefficients for the variables of Eq. 2. Considering that there are two significant internal correlations between independent variables ($F_{21}(HOMO - 2)^*$ with $S_{26}^E(HOMO - 2)^*$ and η_{30} with $S_6^N(LUMO + 2)^*$, see Table 5), the values of R , R^2 , $\text{adj-}R^2$, $F(4,8)$ and SD must be considered with caution. Figure 4 displays the plot of observed vs. calculated $\log(IC_{50})$ values.

Table 4. Beta coefficients and t-test for significance of coefficients in Eq. 2

Var.	Beta	t(8)	p-level
$S_6^N(LUMO + 2)^*$	0.88	19.64	<0.000001
$S_{26}^E(HOMO - 2)^*$	-0.32	-6.86	<0.0001
$F_{21}(HOMO - 2)^*$	0.21	4.45	<0.002
η_{30}	-0.15	-3.34	<0.01

Table 5. Matrix of squared correlation coefficients for the variables in Eq. 2

	$S_6^N(LUMO + 2)^*$	$S_{26}^E(HOMO - 2)^*$	$F_{21}(HOMO - 2)^*$
$S_{26}^E(HOMO - 2)^*$	0.0004	1	0
$F_{21}(HOMO - 2)^*$	0.04	0.31	1
η_{30}	0.23	0.006	0.0009

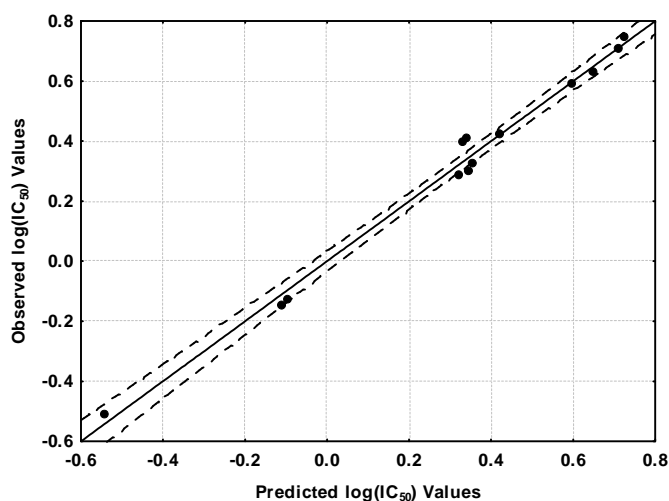


Figure 4. Plot of predicted vs. observed $\log(\text{IC}_{50})$ values (Eq. 2). Dashed lines denote the 95% confidence interval

The associated statistical parameters of Eq. 2 indicate that this equation is statistically significant and that the variation of the numerical values of a group of four local atomic reactivity indices of atoms of the common skeleton explains less than 98% of the variation of $\log(\text{IC}_{50})$ in this series of 1-(4-((2-oxoindolin-3-ylidene)amino)phenyl)-3-arylureas. Figure 4, spanning about 1.4 orders of magnitude, shows that there is a good correlation of observed versus calculated values and that almost all points are inside the 95% confidence interval. This can be considered as an indirect evidence that the common skeleton hypothesis works relatively well for this set of molecules.

Local Molecular Orbitals.

Tables 6-8 show the local MO structure of atoms appearing in Eqs. 1 and 2 (see Fig. XX). Nomenclature: Molecule (HOMO) / (HOMO-2)* (HOMO-1)* (HOMO)* - (LUMO)* (LUMO+1)* (LUMO+2)*.

Table 6. Local molecular orbital structure of atoms 6, 11 and 17

Mol.	Atom 6 (C)	Atom 11 (O)	Atom 17 (C)
1 (93)	91π92π93π-96π97π99	91π92π93π-94π96π100π	91π92π93π-95π97π99π
2 (109)	100π108π109π-113π115π116π	107π108π109π-110π113π115π	107π108π109π-112π114π115π
3 (99)	96π97π99π-100π102π105π	96π97π99π-100π102π106π	95π97π99π-103π104π105π
4 (97)	87π95π97π-101π103π104π	94π95π97π-98π101π104π	94π95π97π-99π100π102π
5 (101)	92π100π101π-105π107π108π	98π100π101π-102π105π107π	98π100π101π-104π105π106π
6 (101)	91π99π101π-105π107π108π	98π99π101π-102π105π107π	98π99π101π-104π105π106π
7 (113)	103π112π113π-117π119π120π	111π112π113π-114π117π119π	111π112π113π-118π119π131π
8 (97)	92π93π94π-98π99π101π	95π96π97π-98π99π102π	92π96π97π-100π101π102π
9 (113)	111π112π113π-117π118π119π	110π112π113π-114π117π118π	111π112π113π-115π116π117π
10 (101)	99π100π101π-104π105π107π	99π100π101π-102π104π105π	99π100π101π-103π105π107π
11 (105)	96π104π105π-109π111π112π	102π104π105π-106π109π111π	102π104π105π-108π110π111π
12 (105)	103π104π105π-109π111π112π	103π104π105π-106π109π111π	103π104π105π-108π110π111π
13 (105)	95π103π104π-108π109π111π	102π103π104π-106π108π109π	103π104π105π-107π109π111π
14 (117)	107π116π117π-121π123π124π	115π116π117π-118π121π123π	115π116π117π-122π123π135π
15 (101)	99π100π101π-103π105π107π	99π100π101π-102π103π105π	99π100π101π-103π104π105π
16 (107)	105π106π107π-111π113π114π	105π106π107π-108π111π113π	104π105π107π-109π110π113π
17 (105)	95π99π103π-107π110π111π	101π103π105π-106π107π110π	102π104π105π-108π109π110π
18 (109)	102π107π109π-111π114π115π	105π107π109π-110π111π115π	106π107π109π-112π113π114π
19 (109)	102π107π109π-111π114π115π	107π108π109π-110π111π115π	106π107π109π-112π114π115π
20 (109)	104π105π106π-110π111π113π	106π107π108π-110π111π113π	102π103π108π-112π113π114π
21 (121)	115π120π121π-125π127π128π	119π120π121π-122π125π128π	119π120π121π-126π127π128π

Table 7. Local molecular orbital structure of atoms 18, 21 and 26

Mol.	Atom 18 (C)	Atom 21 (O)	Atom 26 (C)
1 (93)	91π92π93π-94π95π97π	88π91π92π-94π97π99π	89π92π93π-97π98π99π
2 (109)	106π107σ109π-110π114π115π	104π106π109π-110π112π115π	101π104π106π-111π112π117π
3 (99)	94π95π99π-100π101π103π	97π98π99π-101π109π112π	93π96π98π-101π103π104π
4 (97)	93π94σ97π-98π100π102π	95π96π97π-98π99π100π	88σ91π96π-99π100π103π
5 (101)	98σ100π101π-102π103π104π	99π100π101π-102π103π107π	96π97π99π-103π104π106π
6 (101)	97π98σ101π-102π103π104π	99π100π101π-102π103π107π	92π95π100π-103π104π106π
7 (113)	111σ112π113π-114π118π119π	108π110π113π-114π115π119π	106π107σ110π-115π116π121σ
8 (97)	94π95π96π-98σ100π101π	95π96π97π-104π107π108π	95π96π97π-103π104π110π
9 (113)	110σ111π113π-114π116π117π	111π112π113π-114π115π117π	111π112π113π-115π117π119π
10 (101)	99π100π101π-102π103π104π	97π99π100π-102π105π107π	97π100π101π-105π106π107π
11 (105)	102σ104π105π-106π107π108π	103π104π105π-106π107π111π	100π101π103π-107π108π110π
12 (105)	102σ104π105π-106π107π108π	103π104π105π-106π107π110π	101π103π104π-107π108π110π
13 (105)	102σ103π104π-106π107π109π	103π104π105π-106π109π111π	100σ101π105π-109π110π111π
14 (117)	115σ116π117π-118π122π123π	114π116π117π-118π119π123π	110π111σ114π-119π120π125σ
15 (101)	99π100π101π-102π103π104π	96π99π100π-102π105π107π	98π100π101π-105π106π107π
16 (107)	104σ105π107π-108π110π113π	105π106π107π-108π109π113π	105π106π107π-109π112π116π
17 (105)	102σ103σ105π-106σ108π109π	102σ104π105π-108π110π111π	102σ104π105π-108π109π110π
18 (109)	106π107π109π-110π112π113π	107π108π109π-112π113π114π	104π106π108π-112π113π114π
19 (109)	105π106π109π-110π112π114π	107π108π109π-112π113π114π	105π106π108π-112π113π114π
20 (109)	106π107π108π-110σ112π113π	107π108π109π-114π116π119π	107π108π109π-115π116π126σ
21 (121)	118π119π121π-122π126π127π	119π120π121π-123π126π127π	116π117π119π-123π124π129π

Table 8. Local molecular orbital structure of atoms 27 and 28

Mol.	Atom 27 (C)	Atom 30 (C)
1 (93)	89π92π93π-97π98π99π	89π92π93π-97π98π99π
2 (109)	98π101π106π-111π112π115π	98π101π106π-111π112π117π
3 (99)	96π97π98π-101π104π107σ	95π97π98π-101π103π104π
4 (97)	90π91π96π-99π100π102π	90σ91π96π-99π100π102π
5 (101)	96π97π99π-103π104π106π	96π97π99π-103π104π106π
6 (101)	95π97π100π-103π104π106π	94σ95π100π-103π104π106π
7 (113)	106π107σ110π-115π116π119π	104π106π110π-115π116π121σ
8 (97)	95π96π97π-102π103π104π	94π95π97π-102π103π104π
9 (113)	109π111π112π-115π117π118π	111π112π113π-115π117π118π
10 (101)	99π100π101π-105π106π107π	97π100π101π-105π106π107π
11 (105)	98π101π103π-107π108π110π	100π101π103π-107π108π110π
12 (105)	101π103π104π-107π108π110π	101π103π104π-107π108π110π
13 (105)	101π104π105π-109π110π111π	97π101π105π-109π110π111π
14 (117)	110π111σ114π-119π120π123π	110π111π114π-119π120π125σ
15 (101)	98π100π101π-105π106π107π	99π100π101π-105π106π107π
16 (107)	103π105π106π-109π112π116π	105π106π107π-109π112π116π
17 (105)	101π102σ104π-108π109π110π	101σ102σ104π-109π110π111π
18 (109)	105π106π108π-112π113π114π	105π106π108π-112π113π114π
19 (109)	105π106π108π-112π113π114π	105π106π108π-112π113π115π
20 (109)	107π108π109π-115π116π120σ	107π108π109π-115π116π120σ
21 (121)	112π114σ119π-123π124π126π	116π117π119π-123π124π130π

DISCUSSION

Molecular Electrostatic Potential (MEP).

Figure 5 shows that MEP map of molecule 10 at 4.5 Å of the nuclei.

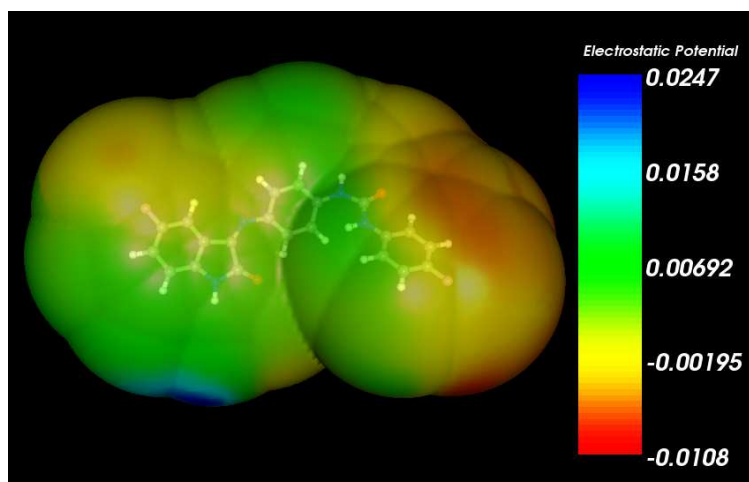


Figure 5. MEP map of molecule 10 at 4.5 Å of the nuclei

We can see that in this extended conformer the MEP map does not show any distinctive feature. As expected, the region around the fluorine atoms has a negative MEP value. To get another view of the MEP, we show in Fig. 6 the MEP map of molecule 10 at isovalues of $|0.01|$.

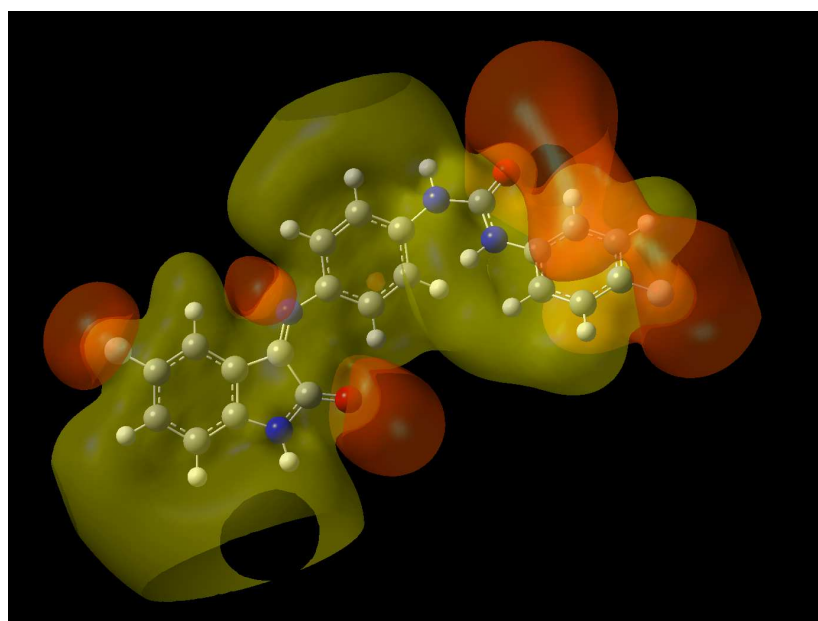


Figure 6. MEP of molecule 10. The orange surface corresponds to negative MEP values (-0.01) and the greenish surface to positive MEP values (0.01)

Here we can distinguish four regions with negative MEP values (see Fig. 2): one close to ring A surrounding the fluorine atom, one surrounding the oxygen atom in ring B, a third one surrounding the nitrogen atom linking rings B and C and a last one surrounding a volume comprising the fluorine atom of ring D, the oxygen atom of the chain linking rings C and D, and part of ring D.

Conformational aspects.

The optimized geometries employed here were obtained for calculations carried out *in vacuo*. We do not know the conformation before and during the interaction with the site(s). Fig. 7 shows the then lowest energy conformers (Dreiding Force Field) of molecule 10.

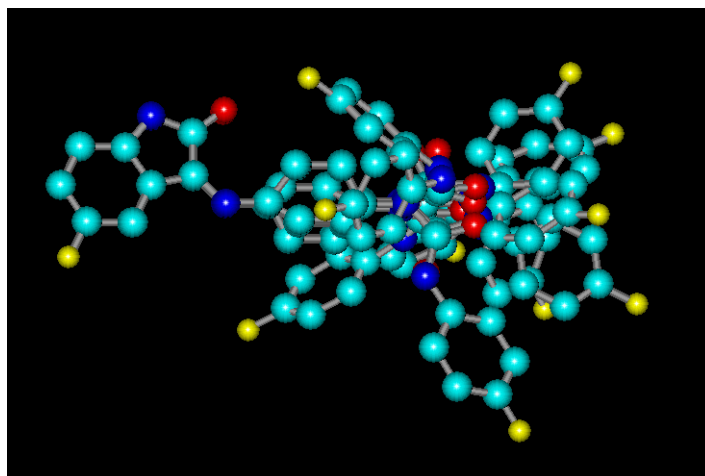


Figure 7. Superimposition of the ten lowest energy conformers of molecule 10

We can see that most conformers are the extended ones but some of them have a closed structure. If we were in possession of information about the microscopic composition of the milieu close to the interaction site we would be able to suggest what the main conformation is. Unhappily, and as far as we know, the interaction site is not known.

Discussion of the results for the *in vitro* cytotoxic activity against HepG2 liver cancer cells.

Table 2 shows that the importance of variables in Eq. 1 is $S_{18}^N(LUMO)^* > F_{18}(HOMO-1)^* > F_{27}(HOMO)^* > S_{11}^E > S_{17}^N(LUMO+2)^*$. A high *in vitro* cytotoxic activity against HepG2 liver cancer cells activity is associated with high (negative) numerical values for S_{11}^E and with low numerical values for $F_{27}(HOMO)^*$ and $F_{18}(HOMO-1)^*$. The case of the nucleophilic superdelocalizabilities will be discussed below. Atom 11 is a carbonyl oxygen in ring B (Fig. 2). A high (negative) value for S_{11}^E indicates that atom 11 is interacting with an electron-deficient center. Atom 17 is a carbon in ring C (Fig. 2). If $S_{17}^N(LUMO+2)^*$ is positive, a high cytotoxicity is associated with high numerical values for this index. To obtain these values, the energy of $(LUMO+2)_{17}^*$ must be shifted downwards, making this MO more reactive. Therefore, we suggest that this MO is interacting with a rich electron center. Table 6 shows that the three lowest vacant local MOs are of π nature, suggesting that the atom-site interaction could be of the π - π kind. Atom 18 is a carbon in ring C (Fig. 2). If $S_{18}^N(LUMO)^*$ is positive, a high cytotoxicity is associated with high numerical values for this index. Also, a low electron population in $(HOMO-1)_{18}^*$ is required for high cytotoxicity. High values of $S_{18}^N(LUMO)^*$ are obtained by shifting downwards the $(LUMO)_{18}^*$ eigenvalue. This indicates that atom 18 is interacting with an electron-rich center through at least its first lowest vacant MO. The requirement of a low electron population in $(HOMO-1)_{18}^*$ could be an indication of a repulsive interaction between occupied MOs of both partners. Atom 27 is a carbon in ring D (Fig. 2). High cytotoxicity is associated with a low value for $F_{27}(HOMO)^*$. This suggests that atom 27 is interacting with an electron-rich center and that $(HOMO)_{27}^*$ is engaged in a repulsive π - π interaction with occupied MOs of the partner because Table 8 shows that $(LUMO)_{27}^*$ has a π nature. Let us notice that despite the fact that all substituents belong to rings A and D, two local atomic reactivity indices belonging to ring C appear in Eq. 1. All the suggestions are displayed in the partial two dimensional (2D) pharmacophore of Fig. 8.

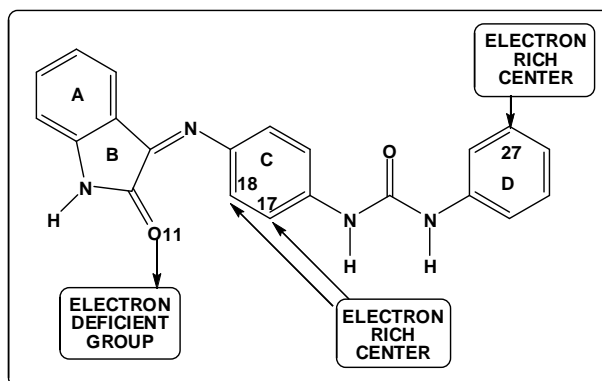


Figure 8. Partial 2D pharmacophore for the *in vitro* cytotoxic activity against HepG2 liver cancer cells by the series of 1-(4-((2-oxoindolin-3-ylidene)amino)phenyl)-3-arylureas

Discussion of the results for the inhibitory activity against VEGFR-2.

Table 4 shows that the importance of variables in Eq. 2 is $S_6^N(LUMO+2)^* \gg S_{26}^E(HOMO-2)^* > F_{21}(HOMO-2)^* > \eta_{30}$. A high inhibitory activity against VEGFR-2 is associated with low values for $S_{26}^E(HOMO-2)^*$ and $F_{21}(HOMO-2)^*$, and with high values for η_{30} . Atom 6 is a carbon in ring A (Fig. 2). If $S_6^N(LUMO+2)^*$ is positive then a high inhibitory activity is associated with low numerical values for this index. Small values are obtained by shifting upwards the energy of the associated eigenvalue. This diminishes the reactivity of $(LUMO+2)_6^*$. We suggest that atom 6 is interacting with an electron-rich center through its first two lowest vacant MOs. These MOs have a π nature (Table 6). Atom 21 is a carbonyl in the chain linking rings C and D (Fig. 2). A low value for $F_{21}(HOMO-2)^*$ seems to be a sign that this MO is engaged in a repulsive interaction with one or more occupied MOs of the site. Therefore, we suggest that atom 21 is interacting with an electron deficient center through its first two highest occupied MOs. Table 7 shows that these MOs have a π nature. Atom 26 is a carbon in ring D (Fig. 2). Small negative numerical values for $S_{26}^E(HOMO-2)^*$ are obtained by shifting downwards the energy of $(HOMO-2)_{26}^*$ and making this MO less reactive. We suggest that atom 26 is interacting with an electron deficient center through its first two highest occupied MOs. Table 7 shows that these MOs have a π nature. Atom 30 is a carbon in ring D (Fig. 2). η_{30} is the energy distance between $(HOMO)_{30}^*$ and $(LUMO)_{30}^*$. Great values for this index are obtained by lowering the $(HOMO)_{30}^*$ energy, rising the $(LUMO)_{30}^*$ or by both procedures. Table 8 shows that, in general, $(LUMO)_{30}^*$ does not coincide with the molecular LUMO, while $(HOMO)_{30}^*$ does coincide with the molecular HOMO. Then, we suggest that atom 30 is interacting with an electron deficient center. All the suggestions are displayed in the partial 2D pharmacophore of Fig. 9.

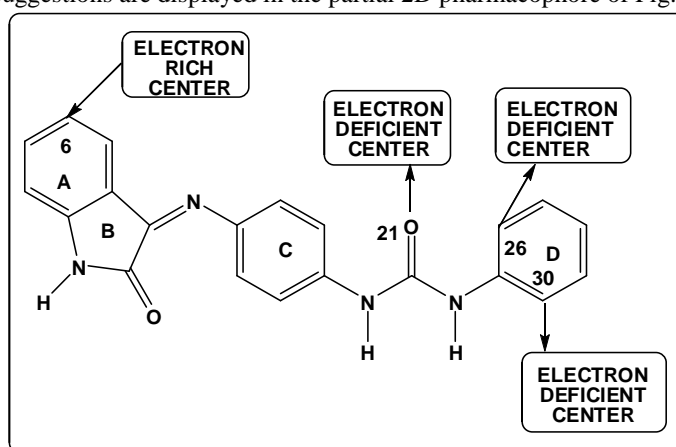


Figure 9. Partial 2D pharmacophore for the inhibitory activity against VEGFR-2 by the series of 1-(4-((2-oxoindolin-3-ylidene)amino)phenyl)-3-arylureas

CONCLUSION

Despite the relatively small numerical range of the experimental data we were able to get information about the center and the possible interactions involved in the inhibition of VEGFR-2 and the cytotoxic activity of the series of 1-(4-((2-oxoindolin-3-ylidene)amino)phenyl)-3-aryureas. This is another example of the ability of the KPG method to study almost any biological activity, provided that the conditions to use it are satisfied. Regarding cytotoxicity, we expect that the accumulation of the data obtained here with previous results will reach a point allowing us to generate a common interaction model.

REFERENCES

- [1] WM Eldehna, M Fares, HS Ibrahim, MH Aly, S Zada, et al., *Eur. J. Med. Chem.*, **2015**, 100, 89-97.
- [2] F-W Peng, J Xuan, T-T Wu, J-Y Xue, Z-W Ren, et al., *Eur. J. Med. Chem.*, **2016**, 109, 1-12.
- [3] SM Abou-Seri, WM Eldehna, MM Ali, DA Abou El Ella, *Eur. J. Med. Chem.*, **2016**, 107, 165-179.
- [4] P Su, J Wang, Y Shi, X Pan, R Shao, et al., *Bioorg. Med. Chem.*, **2015**, 23, 3228-3236.
- [5] S Shen, X Xu, Z Liu, J Liu, L Hu, *Bioorg. Med. Chem.*, **2015**, 23, 1982-1993.
- [6] Y Shan, H Gao, X Shao, J Wang, X Pan, et al., *Eur. J. Med. Chem.*, **2015**, 103, 80-90.
- [7] VA Machado, D Peixoto, R Costa, HJC Froufe, RC Calhelia, et al., *Bioorg. Med. Chem.*, **2015**, 23, 6497-6509.
- [8] W Lu, P Li, Y Shan, P Su, J Wang, et al., *Bioorg. Med. Chem.*, **2015**, 23, 1044-1054.
- [9] H Gao, P Su, Y Shi, X Shen, Y Zhang, et al., *Eur. J. Med. Chem.*, **2015**, 90, 232-240.
- [10] G-R Gao, M-Y Li, L-J Tong, L-X Wei, J Ding, et al., *Chin. Chem. Lett.*, **2015**, 26, 1165-1168.
- [11] YM Abdel Aziz, MM Said, HA El Shihawy, KAM Abouzid, *Bioorg. Chem.*, **2015**, 60, 1-12.
- [12] Z Zhan, J Ai, Q Liu, Y Ji, T Chen, et al., *ACS Med. Chem. Lett.*, **2014**, 5, 673-678.
- [13] C Wang, H Gao, J Dong, Y Zhang, P Su, et al., *Bioorg. Med. Chem.*, **2014**, 22, 277-284.
- [14] Z Tang, S Niu, F Liu, K Lao, J Miao, et al., *Bioorg. Med. Chem. Lett.*, **2014**, 24, 2129-2133.
- [15] L Shi, T-T Wu, Z Wang, J-Y Xue, Y-G Xu, *Bioorg. Med. Chem.*, **2014**, 22, 4735-4744.
- [16] L Shi, T-T Wu, Z Wang, J-Y Xue, Y-G Xu, *Eur. J. Med. Chem.*, **2014**, 84, 698-707.
- [17] MI Shahin, DA Abou El Ella, NSM Ismail, KAM Abouzid, *Bioorg. Chem.*, **2014**, 56, 16-26.
- [18] Y Lv, M Li, T Liu, L Tong, T Peng, et al., *ACS Med. Chem. Lett.*, **2014**, 5, 592-597.
- [19] MLdC Barbosa, LM Lima, R Tesch, CMR Sant'Anna, F Totzke, et al., *Eur. J. Med. Chem.*, **2014**, 71, 1-14.
- [20] E Perspicace, V Jouan-Hureaux, R Ragno, F Ballante, S Sartini, et al., *Eur. J. Med. Chem.*, **2013**, 63, 765-781.
- [21] F Jin, D Gao, Q Wu, F Liu, Y Chen, et al., *Bioorg. Med. Chem.*, **2013**, 21, 5694-5706.
- [22] B Yu, L-d Tang, Y-l Li, S-h Song, X-l Ji, et al., *Bioorg. Med. Chem. Lett.*, **2012**, 22, 110-114.
- [23] KM Amin, SM Abou-Seri, FM Awadallah, AAM Eissa, GS Hassan, et al., *Eur. J. Med. Chem.*, **2015**, 90, 221-231.
- [24] N Filipović, M Stevanović, J Nunić, S Cundrić, M Filipič, et al., *Coll. Surf. B: Biointerf.*, **2014**, 117, 414-424.
- [25] Y O'Callaghan, O Kenny, NM O'Connell, AR Maguire, FO McCarthy, et al., *Biochim.*, **2013**, 95, 496-503.
- [26] F-L Mi, Y-Y Wu, Y-L Chiu, M-C Chen, H-W Sung, et al., *Biomacromol.*, **2007**, 8, 892-898.
- [27] L Chen, Y Zhang, X Kong, S Peng, J Tian, *Bioorg. Med. Chem. Lett.*, **2007**, 17, 2979-2982.
- [28] B Refouvelet, C Guyon, Y Jacquot, C Girard, H Fein, et al., *Eur. J. Med. Chem.*, **2004**, 39, 931-937.
- [29] Note. The results presented here are obtained from what is now a routinary procedure. For this reason, we built a general model for the paper's structure. This model contains *standard* phrases for the presentation of the methods, calculations and results because they do not need to be rewritten repeatedly.
- [30] YC Martin, *Quantitative drug design: a critical introduction*, M. Dekker, New York, **1978**.
- [31] JS Gómez-Jeria, *Int. J. Quant. Chem.*, **1983**, 23, 1969-1972.
- [32] G Klopman, *J. Am. Chem. Soc.*, **1968**, 90, 223-234.
- [33] F Peradejordi, AN Martin, A Cammarata, *J. Pharm. Sci.*, **1971**, 60, 576-582.
- [34] F Tomas, JM Aulló, *J. Pharm. Sci.*, **1979**, 68, 772-776.
- [35] JS Gómez-Jeria, L Espinoza, *Bol. Soc. Chil. Quím.*, **1982**, 27, 142-144.
- [36] JS Gómez-Jeria, D Morales-Lagos, "The mode of binding of phenylalkylamines to the Serotonergic Receptor," in *QSAR in design of Bioactive Drugs*, M. Kuchar Ed., pp. 145-173, Prous, J.R., Barcelona, Spain, **1984**.
- [37] JS Gómez-Jeria, DR Morales-Lagos, *J. Pharm. Sci.*, **1984**, 73, 1725-1728.
- [38] JS Gómez-Jeria, D Morales-Lagos, JI Rodriguez-Gatica, JC Saavedra-Aguilar, *Int. J. Quant. Chem.*, **1985**, 28, 421-428.
- [39] JS Gómez-Jeria, D Morales-Lagos, BK Cassels, JC Saavedra-Aguilar, *Quant. Struct.-Relat.*, **1986**, 5, 153-157.
- [40] JS Gómez-Jeria, BK Cassels, JC Saavedra-Aguilar, *Eur. J. Med. Chem.*, **1987**, 22, 433-437.

- [41] JS Gómez-Jeria, P Sotomayor, *J. Mol. Struct. (Theochem)*, **1988**, 166, 493-498.
- [42] JS Gómez-Jeria, "Modeling the Drug-Receptor Interaction in Quantum Pharmacology," in *Molecules in Physics, Chemistry, and Biology*, J. Maruani Ed., vol. 4, pp. 215-231, Springer Netherlands, **1989**.
- [43] JS Gómez-Jeria, M Ojeda-Vergara, *J. Chil. Chem. Soc.*, **2003**, 48, 119-124.
- [44] JS Gómez-Jeria, *Canad. Chem. Trans.*, **2013**, 1, 25-55.
- [45] JS Gómez-Jeria, M Flores-Catalán, *Canad. Chem. Trans.*, **2013**, 1, 215-237.
- [46] C Barahona-Urbina, S Nuñez-Gonzalez, JS Gómez-Jeria, *J. Chil. Chem. Soc.*, **2012**, 57, 1497-1503.
- [47] A Robles-Navarro, JS Gómez-Jeria, *Der Pharma Chem.*, **2016**, 8, 417-440.
- [48] JS Gómez-Jeria, C Moreno-Rojas, *Der Pharma Chem.*, **2016**, 8, 475-482.
- [49] HR Bravo, BE Weiss-López, J Valdebenito-Gamboa, JS Gómez-Jeria, *Res. J. Pharmac. Biol. Chem. Sci.*, **2016**, in press,
- [50] J Valdebenito-Gamboa, JS Gómez-Jeria, *Der Pharma Chem.*, **2015**, 7, 543-555.
- [51] MS Leal, A Robles-Navarro, JS Gómez-Jeria, *Der Pharm. Lett.*, **2015**, 7, 54-66.
- [52] JS Gómez-Jeria, J Valdebenito-Gamboa, *Der Pharma Chem.*, **2015**, 7, 103-121.
- [53] JS Gómez-Jeria, J Valdebenito-Gamboa, *Res. J. Pharmac. Biol. Chem. Sci.*, **2015**, 6, 203-218.
- [54] JS Gómez-Jeria, J Valdebenito-Gamboa, *Der Pharma Chem.*, **2015**, 7, 323-347.
- [55] JS Gómez-Jeria, J Valdebenito-Gamboa, *Der Pharm. Lett.*, **2015**, 7, 211-219.
- [56] JS Gómez-Jeria, A Robles-Navarro, *Res. J. Pharmac. Biol. Chem. Sci.*, **2015**, 6, 1358-1373.
- [57] JS Gómez-Jeria, A Robles-Navarro, *Res. J. Pharmac. Biol. Chem. Sci.*, **2015**, 6, 1811-1841.
- [58] JS Gómez-Jeria, A Robles-Navarro, *J. Comput. Methods Drug Des.*, **2015**, 5, 15-26.
- [59] JS Gómez-Jeria, A Robles-Navarro, *Res. J. Pharmac. Biol. Chem. Sci.*, **2015**, 6, 755-783.
- [60] JS Gómez-Jeria, A Robles-Navarro, *Der Pharma Chem.*, **2015**, 7, 243-269.
- [61] JS Gómez-Jeria, A Robles-Navarro, *Res. J. Pharmac. Biol. Chem. Sci.*, **2015**, 6, 1337-1351.
- [62] JS Gómez-Jeria, I Reyes-Díaz, J Valdebenito-Gamboa, *J. Comput. Methods Drug Des.*, **2015**, 5, 25-56.
- [63] JS Gómez-Jeria, MB Becerra-Ruiz, *Der Pharma Chem.*, **2015**, 7, 362-369.
- [64] JS Gómez-Jeria, *Res. J. Pharmac. Biol. Chem. Sci.*, **2015**, 6, 688-697.
- [65] MJ Frisch, GW Trucks, HB Schlegel, GE Scuseria, MA Robb, et al., "G03 Rev. E.01," Gaussian, Pittsburgh, PA, USA, **2007**.
- [66] JS Gómez-Jeria, "D-Cent-QSAR: A program to generate Local Atomic Reactivity Indices from Gaussian 03 log files. v. 1.0," Santiago, Chile, **2014**.
- [67] JS Gómez-Jeria, *J. Chil. Chem. Soc.*, **2009**, 54, 482-485.
- [68] JS Gómez-Jeria, *Elements of Molecular Electronic Pharmacology (in Spanish)*, Ediciones Sokar, Santiago de Chile, **2013**.
- [69] Statsoft, "Statistica v. 8.0," 2300 East 14 th St. Tulsa, OK 74104, USA, **1984-2007**.